

Ergoregion instability of exotic compact objects: electromagnetic and gravitational perturbations and the role of absorption

Elisa Maggio^{1,2}, Vitor Cardoso^{2,3}, Sam R. Dolan¹, Paolo Pani⁴

¹ *Consortium for Fundamental Physics, School of Mathematics and Statistics,*

University of Sheffield, Hicks Building, Hounsfield Road, Sheffield S3 7RH, United Kingdom

² *Centro de Astrofísica e Gravitação - CENTRA, Departamento de Física, Instituto Superior Técnico - IST, Universidade de Lisboa - UL, Av. Rovisco Pais 1, 1049-001 Lisboa, Portugal*

³ *Perimeter Institute for Theoretical Physics, 31 Caroline Street North Waterloo, Ontario N2L 2Y5, Canada and*

⁴ *Dipartimento di Fisica, “Sapienza” Università di Roma & Sezione INFN Roma1, Piazzale Aldo Moro 5, 00185, Roma, Italy*

Spinning horizonless compact objects may be unstable against an “ergoregion instability”. We investigate this mechanism for electromagnetic perturbations of ultracompact Kerr-like objects with a reflecting surface, extending previous (numerical and analytical) work limited to the scalar case. We derive an analytical result for the frequency and the instability time scale of unstable modes which is valid at small frequencies. We argue that our analysis can be directly extended to gravitational perturbations of exotic compact objects in the black-hole limit. The instability for electromagnetic and gravitational perturbations is generically stronger than in the scalar case and it requires larger absorption to be quenched. We argue that exotic compact objects with spin $\chi \lesssim 0.7$ ($\chi \lesssim 0.9$) should have an absorption coefficient of at least 0.3% (6%) to remain linearly stable, and that an absorption coefficient of at least $\approx 60\%$ would quench the instability for any spin. We also show that – in the static limit – the scalar, electromagnetic, and gravitational perturbations of the Kerr metric are related to one another through Darboux transformations.

I. INTRODUCTION

Exotic compact objects (ECOs) are under intense scrutiny as probes of near-horizon quantum structures [1–3], as models for exotic states of matter in ultracompact stars [4], and as exotic gravitational-wave (GW) sources that might coexist in the universe along with black holes (BHs) and neutron stars (see Refs. [2, 3] for a recent overview).

The phenomenology of ECOs depends strongly on their compactness (or, equivalently, on the gravitational redshift z at their surface). Objects with $z \sim \mathcal{O}(1)$ (e.g., boson stars [5, 6]) have properties similar to those of neutron stars and display $\mathcal{O}(1)$ corrections in most observables (e.g., multipole moments [7–10], geodesic motion [11], quasinormal mode (QNM) ringing [12–14], tidal Love numbers [15–17], etc.) relative to BHs.

A different class of ECOs (dubbed *ClePhOs* in the terminology introduced in Refs. [2, 3]) is instead associated to modifications of the Kerr metric only very close to the horizon, as in some quantum-gravity scenarios [18–25]. Here then $z \sim \mathcal{O}(10^{20})$ or larger for objects with mass $M \sim 10 M_\odot$ or higher. It is extremely challenging – if not impossible [2, 3, 26] – to rule out or detect these objects through electromagnetic observations, since their geodesic structure is almost identical to that of a BH. On the other hand, GWs emitted by these objects in different scenarios carry unique information on their properties. This includes: (i) GW echoes in the postmerger ringdown phase of a binary coalescence [1, 16] (see also Ref. [27] for an earlier study, and Refs. [28–33] for a debate on the evidence of this effect in aLIGO data); (ii) a (logarithmically-small) tidal deformability that affects the late inspiral [34, 35]; (iii) the absence of tidal heating for ECOs as compared to BHs [35]; (iv) their different spin-induced quadrupole moment [8–10, 36]; and (v) the stochastic GW background from a population of ECOs [37, 38].

In parallel with developing detection strategies for these

signatures, it is also important to assess the viability of ECOs and, in particular, their stability and their formation channels. Spinning ECOs are potentially unstable, due to the so-called *ergoregion instability* [39] (for a review, see Ref. [40]). The latter is an instability that develops in any asymptotically flat spacetime featuring an ergoregion but without an event horizon: since physical negative-energy states can exist inside the ergoregion – a key ingredient in Penrose’s process [41] – it is energetically favorable to cascade toward even more negative states. The only way to prevent such process from developing is by absorbing the negative-energy states. Kerr BHs can absorb radiation very efficiently and are indeed stable even if they have an ergoregion. On the other hand, compact horizonless geometries are generically unstable in the absence of dissipation mechanisms.

The ergoregion instability has been studied for various models [39, 40, 42–48]. The time scale of the instability depends strongly on the spin and on the compactness [49] of the object. In particular, the instability exists only for those objects which are compact enough to possess a photon sphere [40, 50]. The latter is naturally present in all models of ECOs that modify the BH geometry only at the horizon scale, for example by invoking an effective surface located at some Planck distance from the would-be horizon [2, 3].

The ergoregion instability of Planck-inspired ECOs has been recently studied in Ref. [51] for scalar-field perturbations. There, it was shown that, if the ECO interior does not absorb any radiation, the instability time scale is short enough to have a crucial impact on the dynamics of the object. On the other hand, partial absorption (i.e. reflectivity at the object’s surface smaller than unity) may quench the instability completely, just like in the BH case. Because the dissipation of energy in compact objects made of known matter is small, the instability imposes severe constraints on some particular models of horizonless objects [38].

In this paper we extend the analysis of Ref. [51] to elec-

tromagnetic and gravitational perturbations. Since the ergoregion instability is intimately linked to superradiance [40, 52], and since superradiance is enhanced by field spin (at least for rapidly-spinning objects), one expects that the instability gets stronger for gravitational perturbations. Below we quantify this expectation – both by solving the full linear problem numerically and by computing the spectrum of unstable modes analytically in the small-frequency limit – and we discuss the implications of our results for current observational constraints on ECOs.

Any instability is of course also related to the boundary conditions of the problem. While formulating physical boundary conditions for electromagnetic and gravitational fluctuations, we uncovered a curious relation between all sets of perturbations in the static limit: scalar, electromagnetic and gravitational perturbations of the Kerr metric are all related to one another through Darboux transformations. To the best of our knowledge this interesting property of BH perturbations in general relativity has not been reported before. Through this work, we use $G = c = 1$ units.

II. SETUP

A. The canonical ECO

Our setup and methods follow Refs. [38, 51]. We consider a geometry described by the Kerr metric¹ when $r > r_0$ and, at $r = r_0$, we assume the presence of a membrane with some reflective properties. Different models of ECOs are then characterized by different properties of the membrane at $r = r_0$, in particular by a (possibly) frequency-dependent reflectivity. In Boyer-Lindquist coordinates, the line element at $r > r_0$ reads

$$ds^2 = -\left(1 - \frac{2Mr}{\Sigma}\right) dt^2 + \frac{\Sigma}{\Delta} dr^2 - \frac{4Mr}{\Sigma} a \sin^2 \theta d\phi dt + \Sigma d\theta^2 + \left[(r^2 + a^2) \sin^2 \theta + \frac{2Mr}{\Sigma} a^2 \sin^4 \theta\right] d\phi^2, \quad (1)$$

where $\Sigma = r^2 + a^2 \cos^2 \theta$ and $\Delta = r^2 + a^2 - 2Mr$, with M and $J := aM$ the total mass and spin of the object.

Motivated by models of microscopic corrections at the horizon scale, in the following we shall focus on the case

$$r_0 = r_+(1 + \epsilon), \quad 0 < \epsilon \ll 1, \quad (2)$$

where $r_+ = M + \sqrt{M^2 - a^2}$ is the location of the would-be horizon. Although the above parametrization requires $a \leq M$,

the latter condition is not strictly necessary [51]. Note that ϵ is related to the compactness of the object and to the gravitational redshift at the surface, namely $M/r_0 \approx M/r_+(1 - \epsilon)$ and $z \approx \epsilon^{-1/2}(r_+/M - 1)^{-1/2}$. If $r_0 \sim r_+ + l_P$ (where l_P is the Planck length, as suggested by some quantum-gravity inspired models [1–3]) then $\epsilon \sim 10^{-40}$ for a non-spinning object with $M \sim 50 M_\odot$.

B. Linear perturbations

Scalar, electromagnetic, and gravitational perturbations in the exterior Kerr geometry are described in terms of Teukolsky's master equations [55–57]

$$\Delta^{-s} \frac{d}{dr} \left(\Delta^{s+1} \frac{d_s R_{lm}}{dr} \right) + \left[\frac{K^2 - 2is(r-M)K}{\Delta} + 4is\omega r - \lambda \right] {}_s R_{lm} = 0, \quad (3)$$

$$\begin{aligned} & \left[(1-x^2) {}_s S_{lm,x} \right]_{,x} + \left[(a\omega x)^2 - 2a\omega s x + s \right. \\ & \left. + {}_s A_{lm} - \frac{(m+sx)^2}{1-x^2} \right] {}_s S_{lm} = 0, \end{aligned} \quad (4)$$

where ${}_s S_{lm}(\theta) e^{im\phi}$ are spin-weighted spheroidal harmonics, $x \equiv \cos \theta$, $K = (r^2 + a^2)\omega - am$, and the separation constants λ and ${}_s A_{lm}$ are related by $\lambda \equiv {}_s A_{lm} + a^2\omega^2 - 2am\omega$. When $a = 0$, the angular eigenvalues are $\lambda = (l-s)(l+s+1)$. For $a\omega \ll 1$, ${}_s A_{lm}$ can be expanded as [58]

$${}_s A_{lm} = \sum_{n=0} f_{slm}^{(n)} (a\omega)^n, \quad (5)$$

where $f_{slm}^{(n)}$ are expansion coefficients. The above expression provides an excellent approximation whenever $|a\omega| \lesssim 1$, which is always the case for the fundamental modes when $a < M$.

It is convenient to make a change of variables by introducing Detweiler's function [59]

$${}_s X_{lm} = \Delta^{s/2} (r^2 + a^2)^{1/2} \left[\alpha {}_s R_{lm} + \beta \Delta^{s+1} \frac{d_s R_{lm}}{dr} \right], \quad (6)$$

where α and β are certain radial functions. Introducing the tortoise coordinate r_* , defined such that $dr_*/dr = (r^2 + a^2)/\Delta$, the master equation (3) becomes

$$\frac{d_s^2 X_{lm}}{dr_*^2} - V(r, \omega) {}_s X_{lm} = 0, \quad (7)$$

where the effective potential is

$$V(r, \omega) = \frac{U\Delta}{(r^2 + a^2)^2} + G^2 + \frac{dG}{dr_*} \quad (8)$$

where $G = s(r-M)/(r^2 + a^2) + r\Delta(r^2 + a^2)^{-2}$, $U = V_S + \Delta^{-s}(2\alpha' + (\beta'\Delta^{s+1})')/\beta$, $V_S = -[K^2 + is\Delta'K - \Delta(2isK' + \lambda)]/\Delta$, and the prime

¹ The vacuum region outside a spinning object is not necessarily described by the Kerr geometry, due to the absence of an analog to the Birkhoff's theorem in axisymmetry. This implies that the multipolar structure of a spinning ECO might be generically different from that of a Kerr BH. However, in those models that admit a smooth BH limit, there are indications that all multipole moments of the external spacetime approach those of a Kerr BH as $\epsilon \rightarrow 0$ [8–10, 53, 54]. In fact, for $z \rightarrow \infty$, it is natural to expect that the exterior spacetime is extremely close to Kerr, unless some discontinuity occurs in the BH limit.

denotes a derivative with respect to r . The functions α and β can be chosen such that the resulting potential is purely real [59]. In the following we define $R_s = {}_sR_{lm}$, $X_s = {}_sX_{lm}$ and omit the l, m subscripts for brevity.

C. Boundary conditions

By imposing boundary conditions at infinity and at the surface of the ECO, Eq. (7) defines an eigenvalue problem whose eigenvalues, $\omega = \omega_R + i\omega_I$, are the QNMs of the system. In our convention a stable mode corresponds to $\omega_I < 0$, whereas an unstable mode corresponds to $\omega_I > 0$ with instability timescale $\tau := 1/|\omega_I|$.

In order to derive the QNM spectrum, we impose outgoing boundary conditions at infinity [57]

$$X_s \sim e^{i\omega r^*} \quad r \rightarrow \infty. \quad (9)$$

At $r = r_0$ there is a superposition of ingoing and outgoing waves. In general, the boundary condition depends on the properties of the membrane of the ECO. In the following we will focus on the analysis of electromagnetic perturbations of a perfectly reflecting surface, i.e., we shall consider a perfect conductor with electric and magnetic fields that satisfy $E_\theta(r_0) = E_\phi(r_0) = 0$ and $B_r(r_0) = 0$. By writing these conditions in terms of the three complex scalars of the electromagnetic field in the Neuman-Penrose formalism [60], we obtain that the following boundary conditions [40]

$$\partial_r R_{-1} = \left[\frac{iK}{\Delta} - \frac{i}{2K} \left({}_sA_{lm} \pm B + \omega(2ir + a^2\omega - 2am) \right) \right] R_{-1}, \quad (10)$$

where² $B = \sqrt{\lambda^2 + 4m\omega - 4a^2\omega^2}$, the plus and minus signs refer to polar and axial perturbations, respectively.

D. Numerical procedure

Equation (7) with boundary conditions (9) and (10) can be solved numerically through a direct integration shooting method [61]. Starting with a high-order series expansion at large distances, we integrate Eq. (7) [or, equivalently, Eq. (3)] from infinity to $r = r_0$; we repeat the integration for different values of ω until the desired boundary condition at r_0 is satisfied.

The QNMs of the system depend on two continuous dimensionless parameters: the spin $\chi = a/M$ and the parameter ϵ , defined in Eq. (2), that is related to the ECO compactness and to the redshift at the ECO surface. Furthermore, the QNMs depend on three integer numbers: the angular number $l \geq 0$,

the azimuthal number m (such that $|m| \leq l$), and the overtone number $n \geq 0$. For electromagnetic perturbations, we shall focus on the $l = m = 1$ fundamental modes ($n = 0$) which, in the unstable case, correspond to the modes with the largest imaginary part, and thus the shortest instability time scale. In our numerical results, we also make use of the symmetry [62]

$$m \rightarrow -m, \quad \omega_R \rightarrow -\omega_R, \quad {}_sA_{lm} \rightarrow {}_sA_{l-m}^*. \quad (11)$$

The latter guarantees that, without loss of generality, we can focus on modes with $m \geq 0$ only.

III. ECO INSTABILITIES FOR ELECTROMAGNETIC PERTURBATIONS

A. Analytical results: Extension of Vilenkin's calculation to electromagnetic perturbations

Here we extend Vilenkin's analytical computation [42] of scalar perturbations in the background of a perfectly-reflecting Kerr-like object to the electromagnetic case. We use Detweiler's transformation (6) and introduce standard 'in' and 'up' modes, denoted X_s^+ and X_s^- , respectively, with asymptotic behavior

$$X_s^+ \sim \begin{cases} B_+ e^{-i\tilde{\omega} r^*}, & r^* \rightarrow -\infty, \\ e^{-i\omega r^*} + A_+ e^{i\omega r^*}, & r^* \rightarrow \infty, \end{cases} \quad (12a)$$

$$X_s^- \sim \begin{cases} e^{+i\tilde{\omega} r^*} + A_- e^{-i\tilde{\omega} r^*}, & r^* \rightarrow -\infty, \\ B_- e^{+i\omega r^*}, & r^* \rightarrow \infty, \end{cases} \quad (12b)$$

where $\tilde{\omega} = \omega - m\Omega$ and $\Omega = a/(2Mr_+)$ is the angular velocity at $r = r_0$. Since the potential V is real, X_s^\pm and their complex conjugates $X_s^{\pm*}$ are independent solutions to the same equation (7), which satisfy complex conjugated boundary conditions. Via the Wronskian relationships, the coefficients A_\pm and B_\pm satisfy the relations [63]

$$1 - |A_+|^2 = (\tilde{\omega}/\omega) |B_+|^2, \quad (13a)$$

$$1 - |A_-|^2 = (\omega/\tilde{\omega}) |B_-|^2, \quad (13b)$$

and $\tilde{\omega}B_+ = \omega B_-$, from which it follows that $|A_-| = |A_+|$.

We focus on the solution with asymptotics (12b) and we impose the boundary conditions (10) at the surface, i.e., we assume that the latter is a perfect conductor. Near the surface, the function R_{-1} defined in Eq. (10) has the following asymptotics

$$R_{-1} \sim \mathcal{A} \Delta e^{-i\tilde{\omega} r^*} + \mathcal{B} e^{i\tilde{\omega} r^*} \quad r^* \rightarrow -\infty, \quad (14)$$

where $\mathcal{A} = \mathcal{A}_0 + \eta \mathcal{A}_1 + \dots$ and $\mathcal{B} = \mathcal{B}_0 + \eta \mathcal{B}_1 + \dots$, with $\eta \equiv r - r_+$. Since $\Delta \sim (r_+ - r_-)\eta$ near the surface, in Eq. (14) we consider $\mathcal{A} = \mathcal{A}_0$ and $\mathcal{B} = \mathcal{B}_0 + \eta \mathcal{B}_1$ for X_{-1}^- close to the horizon. We then obtain

$$\mathcal{B}_0 = \frac{-2^{1/2}(r_+^2 + a^2)^{1/2}\tilde{\omega}}{B}, \quad (15)$$

$$\mathcal{A}_0 = \frac{-iB}{4K_+ \mathfrak{R}^*} \mathcal{B}_0 A_-, \quad (16)$$

² We notice that the definition of B in [40] has a typo.

where $K_+ = K(r_+)$, $\mathfrak{K} = iK_+ + (r_+ - r_-)/2$ [63]. By inserting Eq. (14) in the Teukolsky equation, we find

$$\mathcal{B}_1 = \left(\frac{iam}{M(r_+ - r_-)} + \frac{2\omega r_+ - i\lambda}{4Mr_+\tilde{\omega}} \right) \mathcal{B}_0. \quad (17)$$

Now Eq. (10) is an equation which relates A_- to the frequency ω , and takes the same form of Eq. (11) in Ref. [42], namely

$$e^{i\tilde{\omega}r_*^0} \mp A_- e^{-i\tilde{\omega}r_*^0} = 0, \quad (18)$$

for the two signs of Eq. (10), respectively, which correspond to polar (−) and axial (+) modes, where $r_*^0 = r_*(r_0)$. Note that the above equation implies that the boundary conditions (10) correspond to Dirichlet and Neumann boundary conditions on the function X_{-1}^- .

Equation (18) implies that

$$\tilde{\omega} = \frac{1}{2|r_*^0|} (p\pi - \Phi + i \ln |A_-|), \quad (19)$$

where p is a positive odd (even) integer for axial (polar) modes and Φ is the phase of the wave reflected at $r = r_0$.

In order to compute the imaginary part of the mode, we first notice that $|A_-| = |A_+|$, so we need to derive $|A_+|$. For waves originated at infinity, X_{-1}^+ has asymptotics (12a). If we express the latter in terms of Teukolsky's function R_{-1} , we find

$$R_{-1} \sim \frac{\mathcal{I}}{r} e^{-i\omega r_*} + \mathcal{R} e^{i\omega r_*} \quad r_* \rightarrow \infty. \quad (20)$$

In the electromagnetic case the amplification factor is defined as [40]

$$Z = \frac{|\mathcal{R}|^2}{|\mathcal{I}|^2} \frac{B^2}{16\omega^4} - 1, \quad (21)$$

where the coefficients of Teukolsky's function R_{-1} are related to the coefficients of X_{-1}^+ by [63]

$$\frac{|\mathcal{R}|^2}{|\mathcal{I}|^2} = \frac{16\omega^4}{B^2} |A_+|^2. \quad (22)$$

It follows that the amplification coefficient reads

$$Z = |A_+|^2 - 1. \quad (23)$$

In the low-frequency regime, the amplification coefficient for generic spin- s waves of frequency ω in a Kerr metric has been computed by Starobinskii [64]

$$Z = -D_{lm} = 4Q\beta_{sl} \prod_{k=1}^l \left(1 + \frac{4Q^2}{k^2} \right) [\omega(r_+ - r_-)]^{2l+1} \quad (24)$$

where $\sqrt{\beta_{sl}} = \frac{(l-s)!(l+s)!}{(2l)!(2l+1)!}$, $Q = \frac{r_+^2 + a^2}{r_+ - r_-} (m\Omega - \omega)$. In particular we will use $Z = -\text{Re}\{D_{lm}\}$ in our calculations since the QNM frequency is complex and $\omega_I \ll \omega_R$.

Finally, the imaginary part of the frequency in Eq. (19) is found from

$$|A_-|^2 - 1 = -\text{Re}\{D_{lm}\}, \quad (25)$$

which is analogous to the Vilenkin relation for scalar perturbations. Note that $Z > 0$ (i.e. $\omega_I > 0$) in the superradiant regime $\omega_R(\omega_R - m\Omega) < 0$. We have therefore shown that electromagnetic unstable modes of a perfectly-reflecting Kerr-like object can be understood in terms of waves amplified at the ergoregion and being reflected at the boundary.

In Appendix A we derive an analogous result using a matched asymptotic expansion. In addition, the latter allows us to compute the phase Φ in Eq. (19) analytically. To summarize, the analytical result valid at small frequency reads³

$$\omega_R \sim -\frac{\pi q}{2|r_*^0|} + m\Omega, \quad (26)$$

$$\omega_I \sim -\frac{2\beta_{sl}M}{|r_*^0|} \left(\frac{r_+}{r_+ - r_-} \right) [\omega_R(r_+ - r_-)]^{2l+1} (\omega_R - m\Omega), \quad (27)$$

where $r_*^0 \sim M[1 + (1 - \chi^2)^{-1/2}] \log \epsilon$ and q is a positive odd (even) integer for polar (axial) modes. Note that in Eq. (27) we left the index s generic because, as we shall argue in the next section, Eqs. (26) and (27) should be valid also for low-frequency gravitational perturbations (as argued in Ref. [2, 3] without proof). Furthermore, we note that the hypothesis of low frequency implies that $M\omega_R \ll 1$. In order to fulfil this condition in the spinning case, it is not sufficient that $\log \epsilon \ll 1$, but also that $M\Omega \ll 1$. Indeed in the BH limit ($\epsilon \rightarrow 0$) we obtain $\omega_R \sim m\Omega$ (hence the frequency is independent on ϵ as long as $\Omega M \gg \epsilon$) and $\omega_I \sim (m\Omega)^{2l+1} / \log^2 \epsilon$. In this limit, the above analytical result is strictly valid only when $\Omega M \ll 1$.

On the other hand, even at high spin the analytical result is accurate near the critical value of the spin such that $\omega_R \approx 0$ and $\omega_I \approx 0$. The above equations predict that the instability occurs when $\omega_R(\omega_R - m\Omega) < 0$ which, for $\epsilon \rightarrow 0$, implies

$$\chi > \chi_{\text{crit}} \approx \frac{\pi q}{m |\log \epsilon|}. \quad (28)$$

Therefore, the critical value of the spin above which the instability occurs can be very small as $\epsilon \rightarrow 0$. However, in the same limit the instability time scale is $\tau \propto \log^2 \epsilon / (m\Omega)^{2l+1}$ [51].

B. Numerical results

Figure 1 shows the agreement between the QNMs computed numerically and analytically through a matched asymptotic expansion. As expected, the agreement is very good in the small-frequency regime, i.e. when both $\log \epsilon$ and ΩM are small.

³ Comparison between Eq. (26) and Eq. (19) reveals that the phase Φ defined in Eq. (19) is a constant and does not depend on the spin. This analytical result is in contrast with the phase computed numerically in Ref. [51]. Since the phase is computed from a matched asymptotic expansion, we believe that the spin dependence of Φ computed in Ref. [51] is due to a different approximation in the calculation. Indeed, in the region near the surface of the ECO, Eq. (A3) of Ref. [51] neglects more terms proportional to $a\omega$ with respect to Eq. (A1).

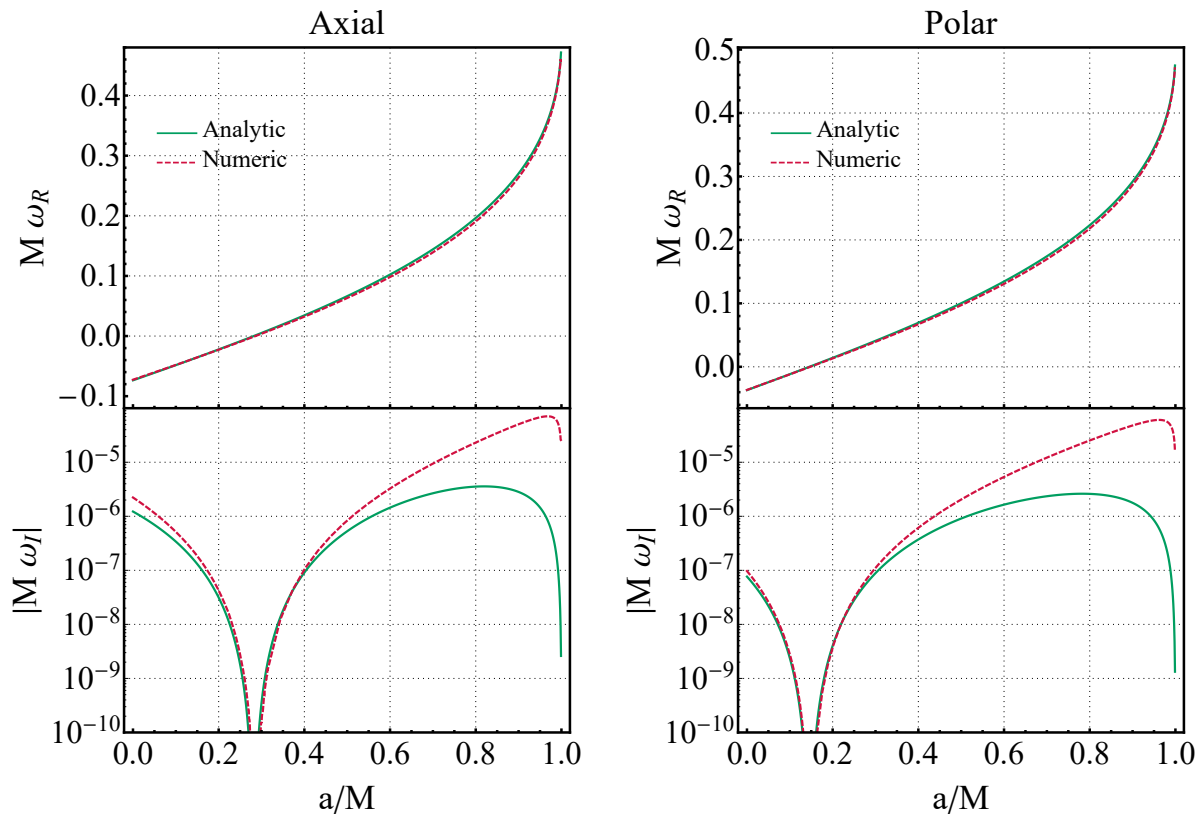


FIG. 1. Real (top panels) and imaginary (bottom panels) part of the fundamental electromagnetic QNM ($l = m = 1, n = 0$) of an ECO as a function of the spin. The left (right) panels refer to axial (polar) modes [corresponding to minus (plus) sign in Eq. (10)], where surface of the ECO is at $r_0 = r_+(1 + \epsilon)$ with $\epsilon = 10^{-10}$. The QNMs computed numerically (dashed curves) are in agreement with the QNMs computed analytically through Eqs. (26)-(27) (continuous curves) when $M\omega \ll 1$.

Notice that both for axial and polar modes the imaginary part of the frequency changes sign for a critical value of the spin, i.e., for $a > a_{\text{crit}}$ the ECO model becomes unstable against the ergoregion instability. An interesting feature is that the threshold of instability is the same both for scalar and electromagnetic perturbations within our numerical accuracy, as shown in Fig. 2. In the next section we explain this fact analytically in terms of Darboux transformations between perturbations of the Kerr metric with different s index. Furthermore, the real part of the scalar QNMs with Dirichlet (Neumann) boundary condition and of the electromagnetic axial (polar) QNMs tends to be the same in the BH limit ($\epsilon \rightarrow 0$), and their imaginary part is also qualitatively similar (see Fig. 2).

We also notice that the axial and polar modes tend to be the same in the BH limit, as it happens for the scalar QNMs with Dirichlet and Neumann boundary conditions in the same limit [51]. Also this feature can be understood analytically by noticing that, as $\epsilon \rightarrow 0$, Eq. (10) reduces to

$$\frac{dR_{-1}}{dr_*} = -i\tilde{\omega}R_{-1}, \quad (29)$$

for both axial and polar modes. Therefore, in the BH limit axial and polar electromagnetic modes of the ECO are isospectral. Given that this is the case for a BH [65], it is natural to conjecture that isospectrality in the BH limit is a generic

feature for any type of perturbation.

IV. STATIC MODES AND DARBOUX TRANSFORMATIONS

The zero-frequency modes are associated with the onset of the ergoregion instability [40, 51, 63], for reflecting boundary conditions. Here we seek a relationship between ϵ , the compactness parameter, and a_{crit} , the critical value of the spin at which the instability appears.

For $\omega = 0$, Teukolsky's equation (3) reduces to the radial equation

$$\Delta^{-s} \frac{d}{dr} \left(\Delta^{s+1} \frac{dR_s}{dr} \right) + \left(\frac{a^2 m^2 + 2is(r-M)am}{\Delta} - \lambda \right) R_s = 0 \quad (30)$$

where $\lambda = (l-s)(l+s+1)$.

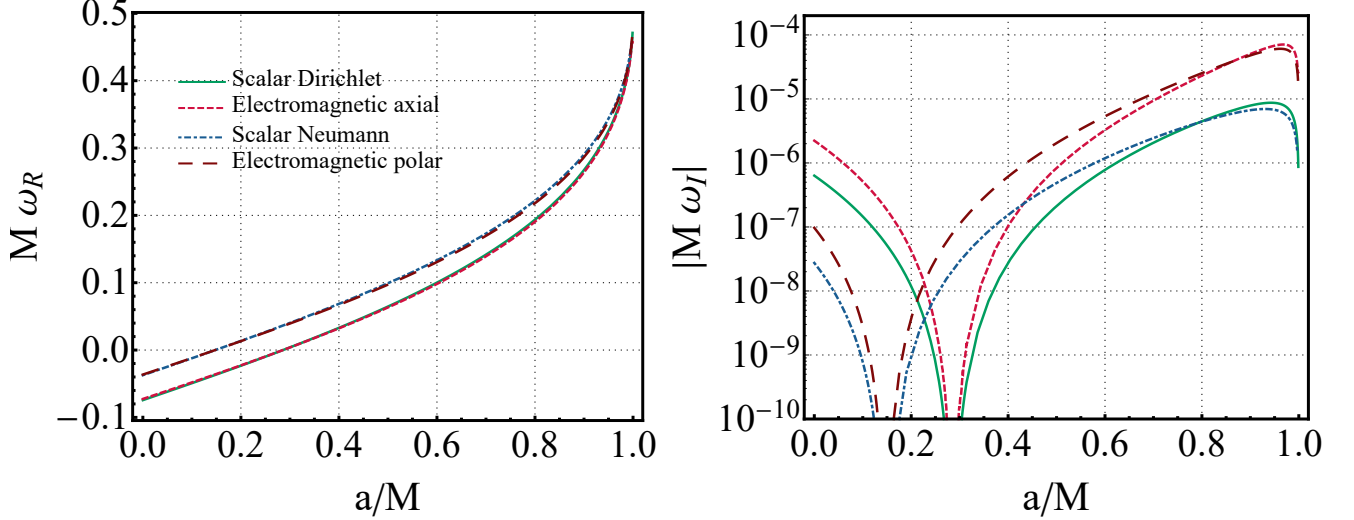


FIG. 2. Real (left panel) and imaginary (right panel) part of the fundamental scalar and electromagnetic QNMs of an ECO as a function of the spin, where the surface of the ECO is at $r_0 = r_+(1 + \epsilon)$ with $\epsilon = 10^{-10}$. The scalar QNMs with Dirichlet (Neumann) boundary condition show a correspondence with the electromagnetic axial (polar) QNMs.

A. Zero frequency modes: scalar field

For $s = 0$, Eq. (30) has the general solution

$$R_0 = c_P P_l^{i\nu}(2x + 1) + c_Q Q_l^{i\nu}(2x + 1), \quad (31)$$

where $\nu \equiv 2am/(r_+ - r_-)$ and $x \equiv (r - r_+)/r_+$. Here $P_l^{i\nu}(\cdot)$ and $Q_l^{i\nu}(\cdot)$ are associated Legendre functions with the branch cut along the real axis from $-\infty$ to 1. The boundary condition of regularity as $r \rightarrow \infty$ imposes that $c_P = 0$. At the surface $r = r_0$, we impose totally-reflecting (Dirichlet or Neumann) boundary conditions. That is,

$$Q_l^{i\nu}(1 + 2x_0) = 0, \quad \text{or} \quad \left. \frac{d}{dx} Q_l^{i\nu}(1 + 2x) \right|_{x=x_0} = 0, \quad (32)$$

where $x_0 = \epsilon r_+/r_+$. By solving Eq. (32) numerically, we obtain the relationship between ϵ and the value of a for which a static mode occurs.

For ultracompact objects characterized by $\epsilon \ll 1$, it is appropriate to use

$$Q_l^{i\nu} \approx \frac{e^{-\pi\nu}}{2\Gamma(i\nu)} \left[x^{-i\nu/2} + \frac{\Gamma(-i\nu)\Gamma(l+1+i\nu)}{\Gamma(i\nu)\Gamma(l+1-i\nu)} x^{i\nu/2} \right] \quad (33)$$

leading to

$$\ln \frac{\epsilon r_+}{r_+ - r_-} \approx -\frac{\pi(p+1)}{\nu} + \frac{i}{\nu} \ln \frac{\Gamma(1-i\nu)\Gamma(l+1+i\nu)}{\Gamma(1+i\nu)\Gamma(l+1-i\nu)}, \quad (34)$$

where p is a non-negative even (odd) integer for Neumann (Dirichlet) modes. This makes it straightforward to find the relationship between $\ln \epsilon$ and $\nu = 2a_{\text{crit}}m/(r_+ - r_-)$, and thus a_{crit} , the critical value of a at the threshold of the ergoregion instability.

Figure 3 shows the zero-frequency modes in the $(\epsilon, a_{\text{crit}})$ domain, for the Neumann (p even) and Dirichlet (p odd)

boundary conditions, for the $l = m$ modes with $m = 1$ (solid), $m = 2$ (dashed) and $m = 3$ (dotted). The plot shows that the ergoregion instability afflicts co-rotating modes of the field. For each $m > 0$ there is a minimum value a_{crit} below which the mode is stable. Let us notice that a_{crit} decreases as m increases, and as ϵ decreases, so that even slowly-rotating ECOs can suffer an ergoregion instability [51], in principle.

In the limit $a \rightarrow 0$ and $\epsilon \rightarrow 0$, Eq. (34) reduces to

$$a_{\text{crit}} \approx \frac{\pi(p+1)}{m|\log \epsilon|} M, \quad (35)$$

which is analogous to Eq. (28) derived analytically in the small-frequency regime. So, for example, a totally reflecting barrier at the Planck scale outside the horizon of a $10M_\odot$ black hole ($\epsilon = l_P/r_+ \sim 5 \times 10^{-40}$) will generate an ergoregion instability in the dipole mode ($m = 1$) if $a \gtrsim 0.035$.

B. Darboux transformations

Now let us consider electromagnetic and gravitational perturbations. It is straightforward to verify that, for $\omega = 0$, the radial functions R_s are related to one another through the following transformations,

$$R_{-1} = R_0 + \frac{i\Delta}{am} R'_0, \quad (36a)$$

$$R_{-2} = \frac{2a^2m^2 - l(l+1)\Delta - 2iam(r-M)}{am(2am - i(r_+ - r_-))} R_0 + \frac{2\Delta(iam + r - M)}{am(2am - i(r_+ - r_-))} R'_0, \quad (36b)$$

defined up to multiplication by a constant factor. Though this relation is not unique, it seems to be the unique transformation

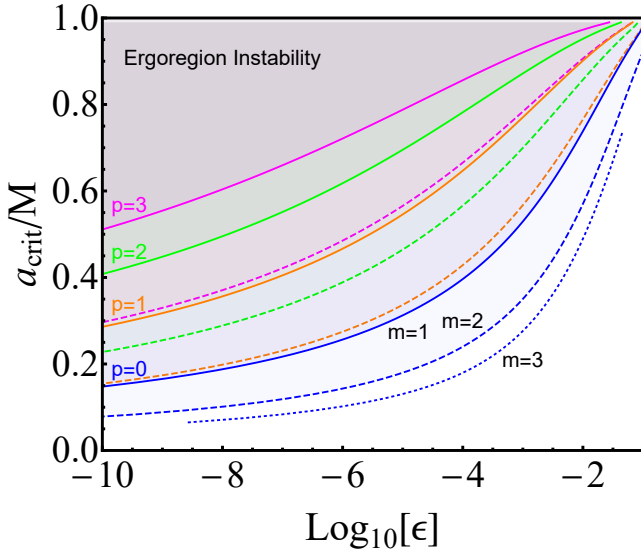


FIG. 3. The ergoregion instability in the ECO spin-compactness parameter space. The lines show the zero-frequency QNMs in the $(\epsilon, a_{\text{crit}})$ domain with Neumann (p even) and Dirichlet (p odd) boundary conditions on the ECO surface at $r_0 = r_+(1 + \epsilon)$. The solid, dashed and dotted lines show the $m = 1, 2$ and 3 modes with $l = m$, respectively. The shaded regions indicate where the corresponding modes suffer the ergoregion instability.

for which the fields are regular at large distances. Equivalent transformations are

$$R_0 = \frac{-iam}{l(l+1)} \left[R'_{-1} + \frac{iam}{\Delta} R_{-1} \right], \quad (37a)$$

$$R_{-2} = \frac{a - 2i(r - M)}{2a + i(r_- - r_+)} R_{-1} + \frac{i\Delta}{2a + i(r_- - r_+)} R'_{-1}. \quad (37b)$$

C. Zero frequency modes: electromagnetic & gravitational perturbations

In the zero-frequency limit, the boundary condition (10) on the electromagnetic wavefunction reduces to

$$R'_{-1} + i \left(\frac{am}{\Delta} - \frac{\varsigma_{\pm} l(l+1)}{am} \right) R_{-1} = 0. \quad (38)$$

where $\varsigma_+ = 1$ for polar modes and $\varsigma_- = 0$ for axial modes. By comparison with Eq. (37a), we see that axial modes are generated from a scalar-field solution with a Dirichlet boundary condition $R_0(r_0) = 0$. For the polar modes, we may take a derivative of (37a) and use the static Teukolsky equation (30) to establish that

$$\Delta R'_0 = \frac{a^2 m^2}{l(l+1)} \left[R'_{-1} + i \left(\frac{am}{\Delta} - \frac{l(l+1)}{am} \right) R_{-1} \right]. \quad (39)$$

Thus, from Eq. (38), the polar modes are generated from a scalar-field solution with a Neumann boundary condition

$$R'_0(r_0) = 0. \quad (4)$$

By virtue of the Darboux transformations, it follows that Eqs. (32) and (34), and Fig. 3, fully describe the zero-frequency modes of, not just a scalar field, but also electromagnetic perturbations for an object with perfectly reflecting boundary conditions. It is natural to posit that this extends to gravitational perturbations as well, for which case one has

$$R'_{-2} = - \left(\frac{(l-1)(l+2)}{2(iam + r - M)} + \frac{iam}{\Delta} \right) R_{-2}, \quad (40a)$$

$$R'_{-2} = - \frac{iam(l-1)(l+2)}{2iam(iam + r - M) + l(l+1)\Delta} R_{-2} - \frac{iam}{\Delta} R_{-2}. \quad (40b)$$

To the best of our knowledge these properties of static perturbations of the Kerr metric have not been presented before. In particular, the above relations show that the $\omega \rightarrow 0$ limit of generic spin- s perturbations is universal.

V. ECO INSTABILITIES FOR GRAVITATIONAL PERTURBATIONS

In principle, gravitational perturbations of our Kerr-like ECO model can be studied by solving Teukolsky's equation (3) [or its alternative version in Detweiler's form (7)] with $s = \pm 2$. However, in this case the issue of boundary conditions is much more subtle (see Ref. [66] for a related discussion). In the electromagnetic case, the boundary conditions (10) are derived by assuming that the object is made of a conducting material, so that the two boundary conditions in Eq. (10) are ultimately related to the requirement that the electric and magnetic field be orthogonal and parallel to the surface, respectively [40]. An analog equation for the gravitational case is currently not available. Furthermore, the boundary condition must depend on the properties of the object's surface, which are also unknown and generically model-dependent.

Nevertheless, we now argue that the analytical results of the previous section can be easily extended to the gravitational case when $\epsilon \rightarrow 0$, at least if the object is perfectly reflecting. Indeed, the previous computation can be easily understood from a “bounce-and-amplify” argument [3, 40], i.e. in terms of quasi-standing waves of a reflecting cavity, slowly leaking out through tunneling in the photon-sphere barrier. The frequency of (co-rotating) modes is set by the width of the cavity, i.e. $\omega_R - m\Omega \sim \pi/r_*^0$, whereas the instability is controlled by the amplification factor Z of the ergoregion at this frequency [40], i.e. $\omega_I \sim Z\omega_R$. This argument does not depend on the boundary conditions at the surface, as long as the object's interior is perfectly reflective, since in this case

⁴ In Ref. [51] the Neumann boundary condition is imposed on the radial wavefunction Y_0 defined as $Y_0 = (r^2 + a^2)^{1/2} R_0$. However, in the small- ϵ limit, the QNM spectrum is analogous to the spectrum obtained by imposing a Neumann boundary condition on R_0 .

the energy is preserved near the surface during subsequent “bounces”.

Another way to look at this effect is to notice that the boundary conditions (10) reduce to Dirichlet and Neumann boundary conditions for the Detweiler function X_s^- . As we have shown, this is true for both scalar ($s = 0$) and electromagnetic ($s = \pm 1$) perturbations. It is now natural to conjecture that the same is true for gravitational perturbations, namely that Dirichlet and Neumann conditions on $X_{\pm 2}^-$ imply perfect reflection at the surface (i.e., no absorption by the interior). With this working assumption, the entire derivation of the previous section follows straightforwardly and the final result in Eqs. (26) and (27) is valid also for low-frequency gravitational perturbations ($s = \pm 2$).

In particular, in the low-frequency limit, the only difference in the instability time scale is given by the term $\beta_{sl}[\omega_R(r_+ - r_-)]^{2l+1}$ in Eq. (27). Since $\beta_{11} = 4\beta_{01}$, the instability time scale for electromagnetic perturbations is simply four times shorter than for scalar perturbations. On the other hand, for gravitational perturbations the dominant mode has $|s| = l = m = 2$, which gives $\beta_{22} = \beta_{11}/25$. Taking into account also the $[\omega_R(r_+ - r_-)]^{2l+1}$ term, in the $\epsilon \rightarrow 0$ limit, we obtain

$$\tau_{222} = \frac{25(1 + \sqrt{1 - \chi^2})^2}{32\chi^2(1 - \chi^2)} \tau_{111}, \quad (41)$$

where $\tau_{slm} = 1/\omega_I$ for a given (s, l, m) . Note that $\tau_{222} > \tau_{111}$ for any spin, showing that the dominant ($l = 2$) gravitational instability is actually *weaker* than the dominant ($l = 1$) electromagnetic instability in the low-frequency limit. This is consistent with the fact that the amplification factor for $s = l = 2$ waves is smaller than that of $s = l = 1$ waves at low frequency [40] (see also Fig. 4 below).

Finally, our conjecture is also supported by the zero-frequency limit discussed in Sec. IV, where we showed that the behavior for scalar, electromagnetic, and gravitational perturbations is universal in the zero-frequency limit.

VI. DISCUSSION: THE ROLE OF ABSORPTION AND ASTROPHYSICAL IMPLICATIONS

Owing to the logarithmic dependence in Eq. (27), the ergoregion-instability time scale for perfectly-reflecting ECOs is always very short, even for Planck-inspired objects with $\epsilon \sim \mathcal{O}(10^{-40})$ [51]. The most natural development of the instability is to remove angular momentum until the superradiant condition is saturated [50]. Thus, spin measurements of dark compact objects indirectly rule out perfectly-reflecting ECOs. Furthermore, the absence of any detectable gravitational-wave stochastic background in LIGO O1 [67, 68] sets the most stringent constraints to date on these models [38].

However, the instability can be totally quenched by (partial) absorption by the object interior [51]. For the case of scalar perturbations, this requires reflectivity $\sim 0.4\%$ smaller than unity [51]. This number corresponds to the maximum superradiant amplification factor for scalar perturbations of a Kerr BH [40, 69] and it is indeed consistent with the “bounce-and-amplify” argument presented in the previous section.

Namely, from Eq. (12b) a right-moving monochromatic wave is backscattered by the ECO potential and acquires a factor $A_- = A_+$. The reflected wave travels to the left and is further reflected at the surface. Let us assume that the reflection coefficient at the object’s surface is $|\mathcal{R}(\omega)|^2$. Then, the left-moving wave $A_+ e^{-i\tilde{\omega}r^*}$ is reflected at the surface as $A_+ \mathcal{R} e^{i\tilde{\omega}r^*}$ (see [70] for a model based on geometrical optics). The process continues indefinitely and the wave acquires a factor $A_+ \mathcal{R}$ for each bounce. Therefore, the condition for the energy in the cavity to grow indefinitely in time is $|A_+ \mathcal{R}|^2 > 1$ or

$$|\mathcal{R}|^2 < \frac{1}{1 + Z}, \quad (42)$$

where both the amplification factor $Z = |A_+|^2 - 1$ and the ECO reflection coefficient $|\mathcal{R}|^2$ are evaluated at the dominant frequency $\omega = \omega_R$. In the low-frequency regime, Z is approximately given by Eq. (24), but it can be computed numerically for any frequency and spin [40, 57]. Since $|\mathcal{R}|^2 \leq 1$, Eq. (42) implies that a necessary condition for the instability is $Z > 0$, i.e. the relevant frequency needs to be in the superradiant regime to trigger the instability. Furthermore, if the object is perfectly reflecting ($|\mathcal{R}|^2 = 1$), the instability is quenched only when $Z < 0$, i.e., only in the absence of superradiance. Likewise, if the object is almost a BH ($\mathcal{R} \approx 0$) the instability is absent for any finite amplification factor Z .

Equation (42) also implies that, to quench the instability completely, it is sufficient that $|\mathcal{R}|^2 < 1/(1 + Z_{\max}) \approx 1 - Z_{\max}$, where Z_{\max} is the maximum amplification coefficient⁵, and the last approximation is valid when $Z_{\max} \ll 1$, as it is typically the case [40, 57].

The above discussion is consistent with the analysis of Ref. [51] for scalar perturbations, but it is actually valid for any kind of perturbations of our ECO model in the BH limit. In general, Eq. (42) implies that the larger the BH amplification factor the larger is the minimum absorption rate necessary to quench the instability. The superradiant amplification factor (and hence the minimum absorption rate required to quench the instability) depends significantly on the spin. This is shown in Fig. 4, where we present $Z(\omega)$ for different values of the spin of a Kerr BH and for different types of perturbations [40, 57]. As predicted by the analytical result, electromagnetic perturbations have the largest amplification factor at low frequency. On the other hand, gravitational perturbations can be amplified much more than electromagnetic or scalar perturbations at high frequency which, by the superradiant condition $\omega(\omega - m\Omega)$ also require highly-spinning objects. The minimum absorption coefficient, $1 - |\mathcal{R}|^2$, required to quench the instability depends strongly on the spin. For an ECO spinning at $\chi \lesssim 0.9$ ($\chi \lesssim 0.7$), an absorption coefficient of at least 6% (0.3%) is sufficient to quench the instability for any type of perturbation. On the other hand, since the maximum superradiance amplification factor is $\approx 138\%$

⁵ A less stringent condition is $|\mathcal{R}(\omega_R)|^2 < 1/(1 + Z(\omega_R))$, where ω_R is the dominant QNM frequency.

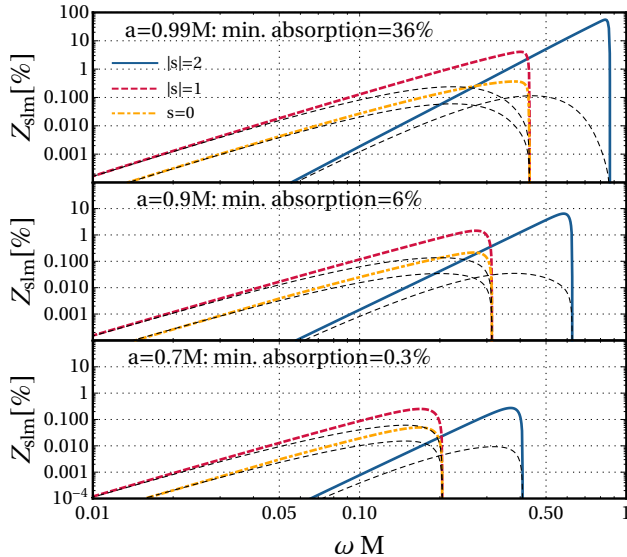


FIG. 4. Superradiant amplification factor for a Kerr BH as a function of the frequency ω of the incident wave for different values of the BH spin and for different types of perturbations (we set $l = m = 1$ for scalar and electromagnetic perturbations, and $l = m = 2$ for gravitational perturbations). The analytical approximation (24) valid at low-frequency (black dashed lines) is compared to the exact numerical result [40, 57]. In each panel we report the minimum absorption coefficient at the ECO surface, $1 - |\mathcal{R}|^2$, necessary to quench the instability, as obtained by saturating Eq. (42).

(for $l = m = 2$ gravitational perturbations of almost extremal BHs [40, 57]), Eq. (42) predicts that an absorption coefficient of at least $\approx 60\%$ would quench the instability in *any* case.

In other words, if a specific ECO can be parametrized by an absorption coefficient of (say) $\approx 1\%$ and it is rapidly spinning when produced (say, $\chi \approx 1$), it would lose angular momentum over a short time scale given by the ergoregion instability, until it reaches a critical value of the spin corresponding to the saturation of Eq. (42). From Fig. 4, in this example the saturation would roughly corresponds to a final spin $\chi \approx 0.8$.

VII. CONCLUSION

We have computed the ergoregion instability for electromagnetic perturbations of a model of Kerr-like ECO, both numerically (for any compactness and spin) and analytically (in the low-frequency regime, which is valid for small spin and in the BH limit). The electromagnetic case is qualitatively similar to the scalar case studied in Ref. [51] but allows us to draw a general picture of the ergoregion instability for ECOs. In particular: (i) we argue that our analytical result can also be extended to the gravitational perturbations of a perfectly-reflecting ECOs in the BH limit; (ii) the instability can be understood in terms of waves trapped within the photon-sphere barrier and amplified by superradiant scattering [40]. Therefore, for any kind of perturbations the instability is completely

quenched if the absorption rate at the ECO surface is at least equal to the maximum superradiance amplification for a given spin- s perturbation of a Kerr BH with same mass and spin.

As a by-product of our analysis, we have also found a set of Darboux transformations that relate the waveforms of $s = 0, \pm 1, \pm 2$ perturbations of the Kerr metric in the static limit. It would be interesting to check whether similar transformations exist also between bosonic and fermionic ($s = \pm 1/2$) perturbations. For the latter there is no superradiance [40] and therefore even highly-spinning, perfectly-reflecting ECOs should be stable against $s = \pm 1/2$ perturbations.

An interesting extension concerns superspinars, i.e. string-inspired, regularized Kerr geometries spinning above the Kerr bound [71]. The ergoregion instability of these models has been studied for scalar perturbations [47, 51] and for gravitational ones [47, 48]. However, in the latter case the boundary conditions adopted do not correspond to Dirichlet or Neumann conditions on the Detweiler function which, as we argued in this work, are the appropriate ones for gravitational perturbations. In light of our results, it would be interesting to extend the stability analysis of superspinars, both for perfectly-reflecting and for partially-absorbing models.

ACKNOWLEDGMENTS

The authors acknowledge networking support by the COST Action CA16104. V. C. acknowledges financial support provided under the European Union's H2020 ERC Consolidator Grant "Matter and strong-field gravity: New frontiers in Einstein's theory" grant agreement no. MaGRATh-646597. P. P. acknowledges the financial support provided under the European Union's H2020 ERC, Starting Grant agreement no. DarkGRA-757480, and and the kind hospitality of the Universitat de les Illes Balears, where this work has been finalized. SD acknowledges financial support from the European Union's Horizon 2020 research and innovation programme under the H2020-MSCA-RISE-2017 Grant No. FunFiCO-777740, and from the Science and Technology Facilities Council (STFC) under Grant No. ST/L000520/1.

Appendix A: Analytical asymptotic matching for electromagnetic perturbations

In this Appendix we derive the analytical QNMs of an ECO under electromagnetic perturbations in the small-frequency regime through a matched asymptotic expansion.

In the region near the surface of the ECO, the radial wave equation (3) reduces to [64]

$$[x(x+1)]^{1-s} \partial_x \left\{ [x(x+1)]^{s+1} \partial_x R_s \right\} + [Q^2 + iQs(1+2x) - \lambda x(x+1)] R_s = 0, \quad (\text{A1})$$

where $x = (r - r_+)/ (r_+ - r_-)$, $Q = (r_+^2 + a^2)(m\Omega - \omega) / (r_+ - r_-)$, and $\lambda = (l - s)(l + s + 1)$. The Eq. (A1) is valid when $M\omega \ll 1$ and it is derived by neglecting the terms proportional to ω in Eq. (3) except for the ones which enter

into Q . The general solution of Eq. (A1) is a linear combination of hypergeometric functions

$$R_s = (1+x)^{iQ} [\alpha x^{-iQ} {}_2F_1(-l+s, l+1+s; 1-\bar{Q}+s; -x) + \beta x^{iQ-s} {}_2F_1(-l+\bar{Q}, l+1+\bar{Q}; 1+\bar{Q}-s; -x)], \quad (\text{A2})$$

where $\bar{Q} = 2iQ$. The large- r behavior of the solution is

$$R_s \sim \left(\frac{r}{r_+ - r_-} \right)^{l-s} \Gamma(2l+1) \left[\frac{\alpha \Gamma(1-\bar{Q}+s)}{\Gamma(l+1-\bar{Q})\Gamma(l+1+s)} + \frac{\beta \Gamma(1+\bar{Q}-s)}{\Gamma(l+1+\bar{Q})\Gamma(l+1-s)} \right] + \left(\frac{r}{r_+ - r_-} \right)^{-l-1-s} \frac{(-1)^{l+1+s}}{2\Gamma(2l+2)} \left[\frac{\alpha \Gamma(l+1-s)\Gamma(1-\bar{Q}+s)}{\Gamma(-l-\bar{Q})} + \frac{\beta \Gamma(l+1+s)\Gamma(1+\bar{Q}-s)}{\Gamma(-l+\bar{Q})} \right], \quad (\text{A3})$$

where the ratio of the coefficients α/β is fixed by the boundary condition at the surface of the ECO.

At infinity, the radial wave equation (3) reduces to [47]

$$r\partial_r^2 f_s + 2(l+1-i\omega r)\partial_r f_s - 2i(l+1-s)\omega f_s = 0, \quad (\text{A4})$$

where $f_s = e^{i\omega r} r^{-l+s} R_s$. The general solution of Eq. (A4) is a linear combination of a confluent hypergeometric function and a Laguerre polynomial

$$R_s = e^{-i\omega r} r^{l-s} [\gamma U(l+1-s, 2l+2, 2i\omega r) + \delta L_{-l-1+s}^{2l+1}(2i\omega r)], \quad (\text{A5})$$

where $\delta = (-1)^{l-s} \gamma \Gamma(-l+s)$ by imposing only outgoing waves at infinity. The small- r behavior of the solution is

$$R_s \sim \gamma r^{l-s} \frac{(-1)^{l-s}}{2} \frac{\Gamma(l+1+s)}{\Gamma(2l+2)} + \gamma r^{-l-1-s} (2i\omega)^{-(2l+1)} \frac{\Gamma(2l+1)}{\Gamma(l+1-s)}. \quad (\text{A6})$$

The matching of Eqs. (A3) and (A6) in the intermediate

region yields

$$\frac{\alpha}{\beta} = -\frac{\Gamma(l+1+s)}{\Gamma(l+1-s)} \left[\frac{R_+ + i(-1)^l (\omega(r_+ - r_-))^{2l+1} L S_+}{R_- + i(-1)^l (\omega(r_+ - r_-))^{2l+1} L S_-} \right], \quad (\text{A7})$$

where

$$R_{\pm} \equiv \frac{\Gamma(1 \pm \bar{Q} \mp s)}{\Gamma(l+1 \pm \bar{Q})}, \quad S_{\pm} \equiv \frac{\Gamma(1 \pm \bar{Q} \mp s)}{\Gamma(-l \pm \bar{Q})}, \quad L \equiv \frac{1}{2} \left(\frac{2^l \Gamma(l+1+s)\Gamma(l+1-s)}{\Gamma(2l+1)\Gamma(2l+2)} \right)^2. \quad (\text{A8})$$

For $s = -1$, the ratio α/β is derived by imposing the boundary conditions (10) in the near-horizon expansion of the solution in the near-horizon region. At the surface, we obtain

$$\frac{\alpha}{\beta} = \mp B^{-1} \bar{Q}(1+\bar{Q})x_0^{\bar{Q}}. \quad (\text{A9})$$

where $x_0 = x(r_0)$, the minus and plus signs refer to polar and axial perturbations, respectively.

By equating Eq. (A7) with Eq. (A9), we obtain an algebraic equation for the complex frequency ω . An approximate solution of ω can be found in the regime $a\omega \ll 1$ and $\epsilon \ll 1$, i.e. $\omega \approx m\Omega$ and $\bar{Q} \ll 1$. Eq. (A7) reduces to $\alpha/\beta = \bar{Q}(1+\bar{Q})/[l(l+1)]$ and in Eq. (A9) $B = l(l+1)$. It follows

$$x_0^{-2iQ} = \mp 1. \quad (\text{A10})$$

By using the tortoise coordinate $r_*^0 = r_*(r_0)$, where $\log(x_0) \sim r_*^0(r_+ - r_-)/(r_+^2 + a^2)$, Eq. (A10) yields

$$e^{-2iQ r_*^0(r_+ - r_-)/(r_+^2 + a^2)} = \mp 1, \quad (\text{A11})$$

which is analogous to Eq. (A18) in Ref. [47] for the scalar-field case. The solution of Eq. (A11) is

$$\omega = -\frac{\pi q}{2|r_*^0|} + m\Omega, \quad (\text{A12})$$

where q is a positive odd (even) integer for polar (axial) modes.

-
- [1] V. Cardoso, S. Hopper, C.F.B. Macedo, C. Palenzuela, and P. Pani, *Phys. Rev.* **D94**, 084031 (2016), arXiv:1608.08637.
[2] V. Cardoso and P. Pani, *Nat. Astron.* **1**, 586 (2017), arXiv:1709.01525.
[3] V. Cardoso and P. Pani, (2017), arXiv:1707.03021.
[4] P. Pani and V. Ferrari, *Class. Quant. Grav.* **35**, 15 (2018), arXiv:1804.01444.
[5] R. Ruffini and S. Bonazzola, *Phys. Rev.* **187**, 1767 (1969).
[6] S.L. Liebling and C. Palenzuela, *Living Rev. Rel.* **15**, 6 (2012), arXiv:1202.5809.
[7] F.D. Ryan, *Phys. Rev.* **D55**, 6081 (1997).
[8] P. Pani, *Phys. Rev.* **D92**, 124030 (2015), arXiv:1506.06050.
[9] N. Uchikata and S. Yoshida, *Class. Quant. Grav.* **33**, 025005 (2016), arXiv:1506.06485.
[10] N. Uchikata, S. Yoshida, and P. Pani, *Phys. Rev.* **D94**, 064015 (2016), arXiv:1607.03593.
[11] P.V.P. Cunha, C.A.R. Herdeiro, E. Radu, and H.F. Runarsson, *Phys. Rev. Lett.* **115**, 211102 (2015), arXiv:1509.00021.
[12] C.B.M.H. Chirenti and L. Rezzolla, *Class. Quant. Grav.* **24**, 4191 (2007), arXiv:0706.1513.
[13] P. Pani, E. Berti, V. Cardoso, Y. Chen, and R. Norte, *Phys. Rev.* **D80**, 124047 (2009), arXiv:0909.0287.
[14] C.F.B. Macedo, P. Pani, V. Cardoso, and L.C.B. Crispino, *Phys. Rev.* **D88**, 064046 (2013), arXiv:1307.4812.
[15] M. Wade, J.D.E. Creighton, E. Ochsner, and A.B. Nielsen, *Phys. Rev.* **D88**, 083002 (2013), arXiv:1306.3901.

- [16] V. Cardoso, E. Franzin, and P. Pani, *Phys. Rev. Lett.* **116**, 171101 (2016), [Erratum: *Phys. Rev. Lett.* 117, no. 8, 089902 (2016)], arXiv:1602.07309.
- [17] N. Sennett, T. Hinderer, J. Steinhoff, A. Buonanno, and S. Ossokine, *Phys. Rev.* **D96**, 024002 (2017), arXiv:1704.08651.
- [18] P.O. Mazur and E. Mottola, (2001), arXiv:gr-qc/0109035.
- [19] S.D. Mathur, *The quantum structure of space-time and the geometric nature of fundamental interactions. Proceedings, 4th Meeting, RTN2004, Kolymbari, Crete, Greece, September 5-10, 2004, Fortsch. Phys.* **53**, 793 (2005), arXiv:hep-th/0502050.
- [20] K. Skenderis and M. Taylor, *Phys. Rept.* **467**, 117 (2008), arXiv:0804.0552.
- [21] A. Almheiri, D. Marolf, J. Polchinski, and J. Sully, *JHEP* **1302**, 062 (2013), arXiv:1207.3123.
- [22] S.B. Giddings, *Phys. Rev.* **D90**, 124033 (2014), arXiv:1406.7001.
- [23] B. Holdom and J. Ren, *Phys. Rev.* **D95**, 084034 (2017), arXiv:1612.04889.
- [24] R. Brustein, A.J.M. Medved, and K. Yagi, *Phys. Rev.* **D96**, 124021 (2017), arXiv:1701.07444.
- [25] C. Barceló, R. Carballo-Rubio, and L.J. Garay, *JHEP* **05**, 054 (2017), arXiv:1701.09156.
- [26] M.A. Abramowicz, W. Kluzniak, and J.P. Lasota, *Astron. Astrophys.* **396**, L31 (2002), arXiv:astro-ph/0207270.
- [27] V. Ferrari and K.D. Kokkotas, *Phys. Rev.* **D62**, 107504 (2000), arXiv:gr-qc/0008057.
- [28] J. Abedi, H. Dykaar, and N. Afshordi, *Phys. Rev.* **D96**, 082004 (2017), arXiv:1612.00266.
- [29] R.S. Conklin, B. Holdom, and J. Ren, (2017), arXiv:1712.06517.
- [30] G. Ashton, O. Birnholtz, M. Cabero, C. Capano, T. Dent, B. Krishnan, G.D. Meadors, A.B. Nielsen, A. Nitz, and J. Westerweck, (2016), arXiv:1612.05625.
- [31] J. Abedi, H. Dykaar, and N. Afshordi, (2017), arXiv:1701.03485.
- [32] J. Westerweck, A. Nielsen, O. Fischer-Birnholtz, M. Cabero, C. Capano, T. Dent, B. Krishnan, G. Meadors, and A.H. Nitz, *Phys. Rev.* **D97**, 124037 (2018), arXiv:1712.09966.
- [33] J. Abedi, H. Dykaar, and N. Afshordi, (2018), arXiv:1803.08565.
- [34] V. Cardoso, E. Franzin, A. Maselli, P. Pani, and G. Raposo, *Phys. Rev.* **D95**, 084014 (2017), arXiv:1701.01116.
- [35] A. Maselli, P. Pani, V. Cardoso, T. Abdelsalhin, L. Gualtieri, and V. Ferrari, *Phys. Rev. Lett.* **120**, 081101 (2018), arXiv:1703.10612.
- [36] N.V. Krishnendu, K.G. Arun, and C.K. Mishra, *Phys. Rev. Lett.* **119**, 091101 (2017), arXiv:1701.06318.
- [37] S.M. Du and Y. Chen, (2018), arXiv:1803.10947.
- [38] E. Barausse, R. Brito, V. Cardoso, I. Dvorkin, and P. Pani, (2018), arXiv:1805.08229.
- [39] J.L. Friedman, *Communications in Mathematical Physics* **63**, 243 (1978).
- [40] R. Brito, V. Cardoso, and P. Pani, *Lect. Notes Phys.* **906**, pp.1 (2015), arXiv:1501.06570.
- [41] R. Penrose, *Nuovo Cimento.J. Serie I*, 252 (1969).
- [42] A. Vilenkin, *Phys. Lett.* **78B**, 301 (1978).
- [43] N. Comins and B.F. Schutz, *Proceedings of the Royal Society of London Series A* **364**, 211 (1978).
- [44] S. Yoshida and Y. Eriguchi, *MNRAS* **282**, 580 (1996).
- [45] K.D. Kokkotas, J. Ruoff, and N. Andersson, *Phys.Rev.* **D70**, 043003 (2004), arXiv:astro-ph/0212429.
- [46] V. Cardoso, P. Pani, M. Cadoni, and M. Cavaglia, *Phys. Rev.* **D77**, 124044 (2008), arXiv:0709.0532.
- [47] V. Cardoso, P. Pani, M. Cadoni, and M. Cavaglia, *Class. Quant. Grav.* **25**, 195010 (2008), arXiv:0808.1615.
- [48] P. Pani, E. Barausse, E. Berti, and V. Cardoso, *Phys. Rev.* **D82**, 044009 (2010), arXiv:1006.1863.
- [49] C.B.M.H. Chirenti and L. Rezzolla, *Phys. Rev.* **D78**, 084011 (2008), arXiv:0808.4080.
- [50] V. Cardoso, L.C.B. Crispino, C.F.B. Macedo, H. Okawa, and P. Pani, *Phys. Rev.* **D90**, 044069 (2014), arXiv:1406.5510.
- [51] E. Maggio, P. Pani, and V. Ferrari, *Phys. Rev.* **D96**, 104047 (2017), arXiv:1703.03696.
- [52] R. Vicente, V. Cardoso, and J.C. Lopes, *Phys. Rev.* **D97**, 084032 (2018), arXiv:1803.08060.
- [53] K. Yagi and N. Yunes, *Phys. Rev.* **D91**, 123008 (2015), arXiv:1503.02726.
- [54] K. Yagi and N. Yunes, *Phys. Rev.* **D91**, 103003 (2015), arXiv:1502.04131.
- [55] S.A. Teukolsky, *Phys. Rev. Lett.* **29**, 1114 (1972).
- [56] S.A. Teukolsky, *Astrophys.J.* **185**, 635 (1973).
- [57] S.A. Teukolsky and W.H. Press, *Astrophys. J.* **193**, 443 (1974).
- [58] E. Berti, V. Cardoso, and M. Casals, *Phys.Rev.* **D73**, 024013 (2006), arXiv:gr-qc/0511111.
- [59] S. Detweiler, *Proceedings of the Royal Society of London Series A* **352**, 381 (1977).
- [60] A.R. King, *Mathematical Proceedings of the Cambridge Philosophical Society* **81**, 149 (1977).
- [61] P. Pani, *Proceedings, Spring School on Numerical Relativity and High Energy Physics (NR/HEP2), Int. J. Mod. Phys.* **A28**, 1340018 (2013), arXiv:1305.6759.
- [62] E.W. Leaver, *Proc. Roy. Soc. Lond.* **A402**, 285 (1985).
- [63] M. Casals and A.C. Ottewill, *Phys. Rev. D* **71**, 124016 (2005).
- [64] A.A. Starobinskij and S.M. Churilov, *Zhurnal Eksperimentalnoi i Teoreticheskoi Fiziki* **65**, 3 (1973).
- [65] S. Chandrasekhar, *The Mathematical Theory of Black Holes* (Oxford University Press, New York, 1983).
- [66] R.H. Price and G. Khanna, *Class. Quant. Grav.* **34**, 225005 (2017), arXiv:1702.04833.
- [67] B.P. Abbott *et al.* (Virgo, LIGO Scientific), *Phys. Rev. Lett.* **116**, 131102 (2016), arXiv:1602.03847.
- [68] B.P. Abbott *et al.* (Virgo, LIGO Scientific), *Phys. Rev. Lett.* **118**, 121101 (2017), arXiv:1612.02029.
- [69] W.H. Press and S.A. Teukolsky, *Nature* **238**, 211 (1972).
- [70] A. Testa and P. Pani, (2018), arXiv:1806.04253.
- [71] E.G. Gimon and P. Horava, *Phys. Lett.* **B672**, 299 (2009), arXiv:0706.2873.